

A new proposed method for observing fluid in rock fractures using the enhanced X-ray image of digital radiography

Huan Sun (✉ sunhuan@hainanu.edu.cn)

Hainan University <https://orcid.org/0000-0002-9825-7036>

Qijian Long

Hainan University

Xiaoli Liu

Tsinghua University

Zhenni Ye

Hainan University

Enzhi Wang

Tsinghua University

Weisheng Du

China Coal Research Institute

Research Article

Keywords: fluid in rock fractures enhanced X-ray imaging of digital radiography (EXIDR), pipe rupture, seepage and diffusion, mean square flow.

Posted Date: May 7th, 2021

DOI: <https://doi.org/10.21203/rs.3.rs-504488/v1>

License: © ⓘ This work is licensed under a Creative Commons Attribution 4.0 International License.

[Read Full License](#)

A new proposed method for observing fluid in rock fractures using the enhanced X-ray image of digital radiography

Corresponding Author 1#: Huan Sun

Title: Associate professor

Affiliation: School of Civil Engineering and Architecture, Hainan University, Haikou, Hainan, 570228, China.

E-mail: sunhuan@hainanu.edu.cn

Corresponding author ORCID: [0000-0002-9825-7036](https://orcid.org/0000-0002-9825-7036)

Author 2#: Qijian Long

Title: Master

Affiliation: School of Civil Engineering and Architecture, Hainan University, Haikou, Hainan, 570228, China.

E-mail: lqqq123@qq.com

Co-Corresponding Author 3#: Xiaoli Liu

Title: Associate professor

Affiliation: State Key Laboratory of Hydrosience and Engineering, Tsinghua University, Beijing, 100084, China.

E-mail: xiaoli.liu@mail.tsinghua.edu.cn

Author 4#: Zhenni Ye

Title: Doctor

Affiliation: School of Civil Engineering and Architecture, Hainan University, Haikou, Hainan, 570228, China.

E-mail: zn.ye@hainanu.edu.cn

Author 5#: Enzhi Wang

Title: Professor

Affiliation: State Key Laboratory of Hydrosience and Engineering, Tsinghua University, Beijing, 100084, China.

E-mail: nzawang@mail.tsinghua.edu.cn

Author 6#: Weisheng Du

Title: Doctor

Affiliation: Deep Mining and Rock Burst Research Institute, China Coal Research Institute, Beijing 100013, China.

E-mail: duweisheng1225@126.com

Abstract: Fluid in rock fractures always continually induces geo-catastrophe in water-rock system engineering. Intuitively observing fluid in fractures is the key method to reveal interaction mechanism of the water-rock under different engineering background, and provide some insights for solving engineering issues. This study proposes the visual method of fluid in rock fractures using enhanced X-ray image digital radiography (EXIDR), and carries out the coupled hydro-mechanical tests on the basis of the material scale of carbonate rocks, red bed mudstone (RBM) and coals. The experimental results show the transition mechanism of pipe flow (PF) to fissure flow (FF) during carbonate rock failures. The flow regime has undergone an evolution process from laminar flow to turbulent flow, also of this change with the fractal characteristics of PF-FF in carbonate rocks under multilevel stress loading. Also, the damage coefficient of RBM under coupled hydrodynamics and multilevel stress loading is non-linearly increasing. Therefore, the initial permeability of RBM under hydrodynamics is significant for geo-hazards prevention in the engineering, which are induced by the seepage and diffusion effects. Besides, the mean square flow (MSF) describes the flow rate varies as the fracture growth and extension, i.e. the fractional exponential evolution law that has a transition changes from super-diffusion flow to sub-diffusion flow. This indicates that fluid in fractures show the double behaviors of anomalous diffusion and nonlinear flow during coal and rock failures.

Keywords: fluid in rock fractures enhanced X-ray imaging of digital radiography (EXIDR), pipe rupture, seepage and diffusion, mean square flow.

1. Introduction

The water-rock interaction theory that between geological structures and geofluids is a fundamental problem in many engineering fields with respect to the engineering geology, hydraulic engineering and mining et al, more specifically, Karst mountain instabilities ([Adji and Bahtiar 2016](#); [Gao et al. 2020](#)), groundwater bursting in the coal mine ([Wu et al. 2004](#); [Yao et al. 2016](#)), and landslides in RBM regions ([Zhang et al. 2015](#)), etc. These disasters all have the common scientific problems relating to the seepage and defects of rocks. It is a challenge tasks of rock mechanics that intuitively observing behavior of rock deformation, disruption and seepage. That is also the inevitable development of transparent geology in the study area of the Earth Science and Technology. In recent years, some theoretical and technical research make progress aspects of in-situ stress field, fracture field and seepage field of visualization technologies, such as 3D printing ([Watson et al. 2019](#); [Zhu et al. 2018](#)), stress freezing ([Ju et al. 2021](#)), fractal reconstruction ([Zhou and Xiao 2018, 2019](#)), and nuclear magnetic resonance (NMR) ([Zhao et al. 2010](#)). Many published results of fluids in fractures focus on the Darcy or non-Darcy laws ([Wang et al. 2016](#)), cubic laws ([Liu et al. 2017](#); [Xie et al. 2015](#)) and its modifications ([Wang et al. 2018](#)), Forchheimer Equation of fracture networks seepage and numerical simulations ([Xiong et al. 2019; 2020](#)). The surface roughness of fractures is very complex with the aperture variability, and it is not applicable for the more precision requirements. Therefore, it is the previous task of quantitatively describing flow in rock fractures that the roughness degree and the geometric irregularity of fractures ([Barton et al. 1985](#)). Fractal dimension is a mathematical index to quantify the complexity of rock fractures ([Ghosh and Daemen 1993](#)). In this regard, Ju et al. ([2013](#)) put forward the fractal permeability coefficient of single rough fracture and established the quantitative relationship between the fractal dimension of single rock fracture and its hydro-property. In regard to rock structure, fracture networks, hydro-conductivity of fracture, damage and seepage of rocks ([Shahbazi et al. 2020](#); [Sun et al. 2020b](#)), Chen et al. ([2014](#)) proposed the hydraulic model coupled of non-linear deformation and unsteady seepage of rocks. Liu et al.

(2008) put forward a coupled model of seepage-stress on the basis of discontinuous deformation and discrete fracture networks. However, flow rate of rock fractures would be an inertial range with the crack propagation, damage intensifying and flow velocity increasing gradually (Xiong et al. 2019; 2020). Meanwhile, the cubic law is inapplicable for describing fracture flow (Lavrov 2014; Zimmerman and Bodvarsson 1996). Forchheimer equation is proposed to describe the nonlinear relationship between flow velocity and pressure gradient, i. e. $-\nabla P = AQ + BQ^2$, where A is the coefficient of linear flow and B is the coefficient of nonlinear flow (Rong et al. 2017). A and B all are related to fracture roughness, geometry and so on. In this regard, Rong et al. (2018) presents the hydro-rock coupling model of fracture and shear deformation based on the Forchheimer equation. Liu et al. (2020) carried out the related theoretical and numerical simulation on nonlinear flow mechanism of fracture network in deep rocks. The evolution of seepage behavior in rock mass is closely related to the damage parameters. The seepage coupled damage model can be used to effectively evaluate the stability of rock mass in the engineering (Wang et al. 2015). In fact, geofluids flows always show the dual mechanical behavior of non-linear flow and anomalous diffusion phenomenon together with the growth and extension of rock fractures (Chechkin et al. 2005; Raghavan 2011; Wang et al. 2019). This is the essential reason of the non-linear catastrophe that induced by fluid flow in fractures during excavation engineering of water-rock system.

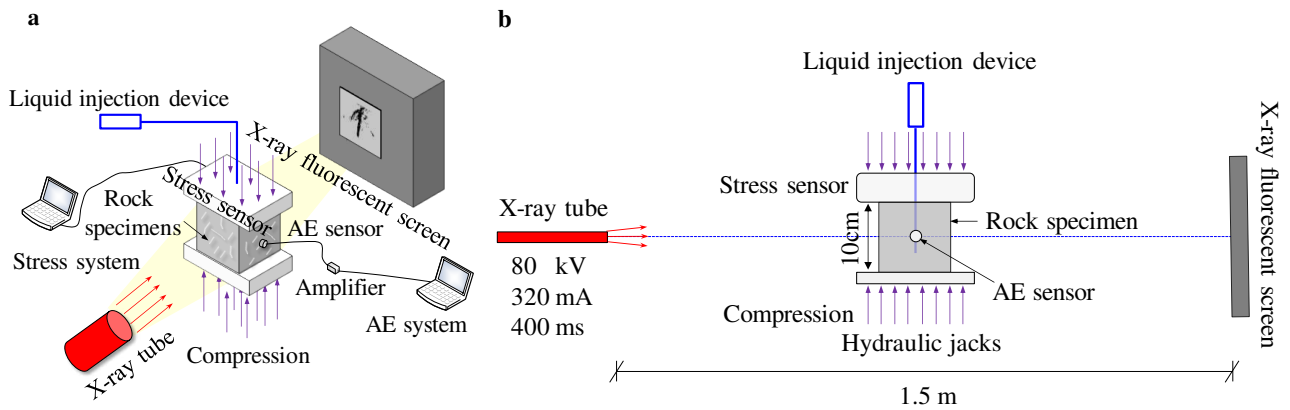
The X-ray radiography has greatly promoted the further development in all aspects of study fields. The commonly used medical or industrial X-ray computer tomography (CT) scanning (Hirono et al. 2003), and its post-processing systems can vividly realize three-dimensional reconstruction for the real internal structures using volume data and algorithms. Therefore, the reconstruction mainly relies on the volume data obtained from X-ray CT scanning, which is the fundamental prerequisite for visualizing fracture and fluid media in rocks. On the basis of this principle, this study proposes a new method of using medical cardiovascular and enhanced X-ray imaging digital radiography to observe the water medium replaced by injecting contrast agent or iodine agent in rock fractures. Then, X-ray images of fluids in rock fractures can be printed, which provides data basis for further to study on the hydro-mechanics interaction with rock failures. Hence, samples of carbonate rocks, RBM and coal are separately carried out to test hydro-properties differences of rock materials. Experimental data of stress, acoustic emission (AE), water flow rate and X-ray images can be achieved. On the basis of these data, fluid catastrophe in different rock engineering would be recognized with analyzing the dual mechanical behaviors of fluids flow and anomalous diffusion. This will provide some new ideas and guidance for geofluids catastrophe and geo-disasters prevention.

2. Fluid visualization in rock fractures using EXIDR

2.1 Loading device matching with the X-ray CT or DR system

In order to continuously shoot the morphology evolutions of fluid in fractures during rock specimens failure, the multi-level stress loading device is designed (Sun et al. 2019), and developed for matching the medical X-ray DR system. The testing system is composed of a stress monitoring system, an AE testing system and an image capturing system. The design principle of the experimental testing system is shown in Figure 1. This experiment aims to obtain fluid images and mechanic properties during rock failures with loading steps. The mechanical design of loading device is shown in Figure 2. The size of device has a height of 500mm and a width of 314mm, which is mainly composed of three carrier plates and connecting rods that is made of Q235 steel materials. The Nylon

sleeves are set as connecting rods aiming to slide smoothly. The middle plate can be placed on a cube specimen size of 100mm. The spoke sensor aiming to stress monitoring is installed at the bottom of the upper plate. The hydraulic jack aiming to push the middle plate is installed at the lower plate. The bottom of fluid director is designed at the middle plate to meet the diversion and leakage requirements. The distance between the X-ray tube and the target board is 1.5m. The hydraulic jack of 30T is used to produce multi-level loading by controlling of the handle and watching the digital display. The loading process is synchronized with the stress monitoring, AE monitoring and the pipe flow monitoring.



(a) Three-dimensional schematic of the design principle (b) Sectional schematic of the design principle
 Figure 1 Principle of observing fluid in rock fractures using EXIDR

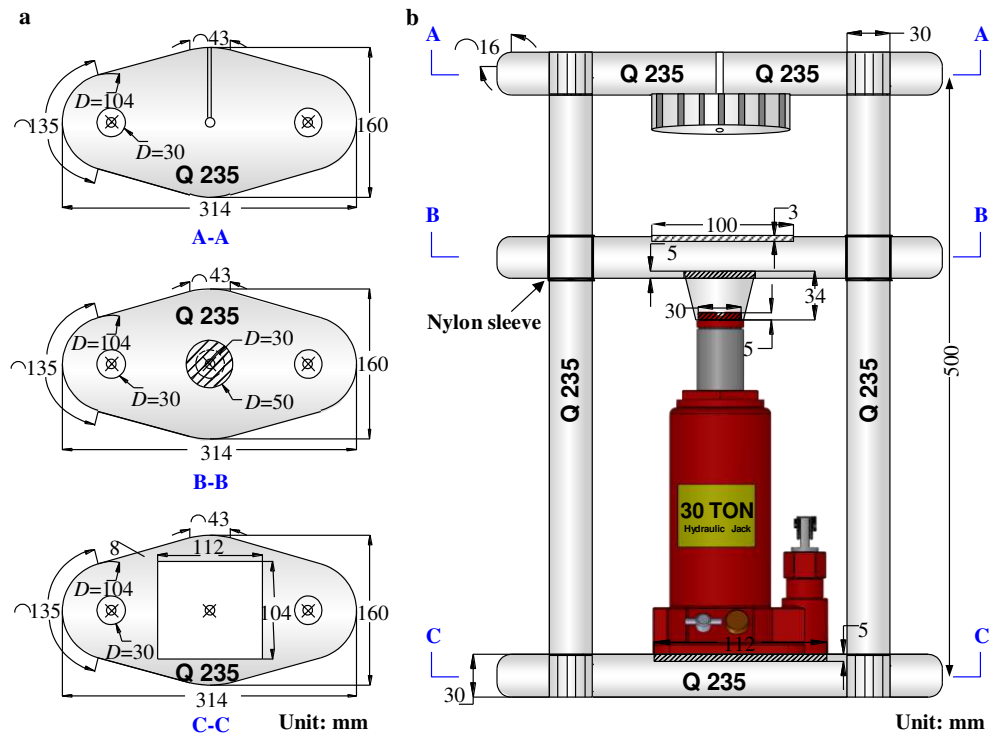
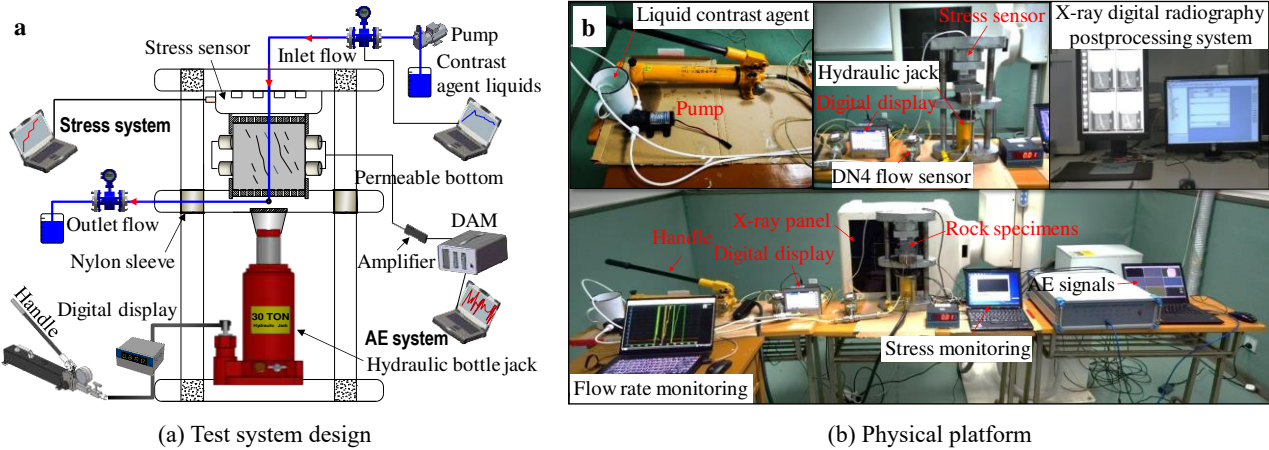


Figure 2 Design of multi-level loading device matching with X-ray DR or CT system

The testing system is installed with the self-priming pump (LS-0412) of 15W to inject contrast fluid (see Figure 3a), the range of spoke sensor is greater than 30T (see Figure 3b), and the DN4 flow meter can collect the changes of the flow rate with the pipe rupture in rocks. Also, AE monitoring technology is used to quantify the degree of rock failures. The experiment system and physical platform are shown in Figure 4.



(a) Self-priming pump of LS-0412 (b) Stress sensor (c) Flow sensor of DN4
Figure 3 Monitoring components for the testing platform system



(a) Test system design (b) Physical platform
Figure 4 Physical platform and testing system of observing fluid in rock fractures using EXIDR

2.2 Samples collection and specimens preparation

The method proposed in this study aims to explore the evolution behaviors of fluid in fractures based on the block scale of rock material. Therefore, the size of cubic specimens is no less than $5\text{cm} \times 5\text{cm} \times 5\text{cm}$ (length \times width \times height) by cutting method to prepare tests and take a hole at the center of specimens to form a diversion channel. A total of 9 specimens of carbonate rocks (size of $7\text{cm} \times 7\text{cm} \times 7\text{cm}$ and $10\text{cm} \times 10\text{cm} \times 10\text{cm}$), 4 specimens of RBM rocks (size of $10\text{cm} \times 10\text{cm} \times 10\text{cm}$) and 16 specimens of coal-rocks (size of $10\text{cm} \times 10\text{cm} \times 10\text{cm}$) are prepared for the experimental project, as shown in Figure 5. Carbonate rock specimens are numbered from KR-01 to KR-09, red bed mudstone specimens are numbered from RBM-01 to RBM-04, and coal-rock specimens of overlying stratum are numbered from CSOS-01 to CSOS-11, RSOS-01 to RSOS-05.



(a) Karst rock specimen (b) red bed mudstone specimen (c) Coal rock specimen

Figure 5 Standard preparations of rock specimens of different lithology

2.3 Testing steps and data analysis methods

This test aims to observe fluids flow in fractures with the rock failures as well as obtaining multi-index of the stress, AE signals, and flow rate, etc. The X-ray images are taken while loading on rock specimens. The test step is shown in Figure 6. According to the test data, pipe flow rate correlated with the rock parameters as the time duration, which shown in Figure 7. Meanwhile, morphological features of liquids flow in fractures quantitatively

extracted from X-ray images using methods of the fractal dimension, cluster segmentations and threshold segmentations. These quantitative results are connected with the theoretical equations such as cubic law, Darcy or non-Darcy laws, Fick diffusion. Then, some physical control equations are given so as to describe the geological disasters that induced by fluid filling fractures in the engineering. Also, the physical phenomenon of geo-disasters will be revealed by inferring from the hydro-properties of rock materials, which is of great significance to provide some guidance for geo-hazards prevention of gas hydrate extraction, landslides and mining, etc.

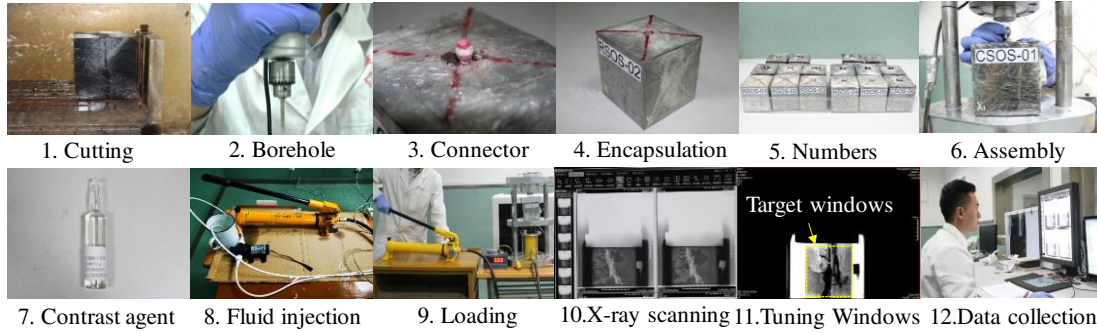


Figure 6 Experiment steps of visualization fluid in fractures during rock failures using X-ray digital radiography.

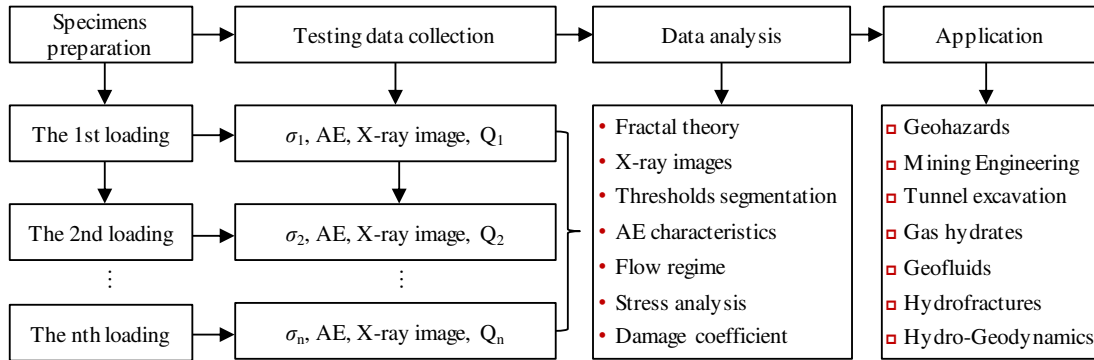


Figure 7 Fracture fluid evolution analysis method and application field during rock fracture

3. Theory of geohazards induced by fluid in rock fractures

3.1 Transition mechanism of pipe-fissure flow during karst rock failures

The rock mass of Karst Mountain is the multi-media that composed of pipelines, fractures and porous, which is an important channel carrier of underground water flow. The hydro-dynamics of underground water is different from the static seepage of pores-fracture in karst rocks. Pores and fractures occupy the main part of the inner space in carbonate rock mediums. Especially, the nonlinear flow of fluids in fractures and pipelines play a role in the evolution of the Karst hydrodynamic system (Sun et al. 2021). Therefore, this paper proposes a new visual method of flow distributions during carbonate rock failures, to explore the flow regime with pipe rupture in rocks. The experiment results from the pipe flow regime can provide some precursor insights for the prediction of karst landslide. A total of 9 rock specimens are prepared for the experiment, of which only 4 rock specimens are success to obtain the completed data. The specimens are numbered KR-01 to KR-04, and the inlet flow rate and outlet flow rate of the pipe rupture are collected in the experiment progress. Reynolds number of PF is calculated with Equation 1 and the flow regime variation of PF is shown in Figure 8.

$$\begin{cases} Re = \frac{\rho v d}{\eta} \\ Q = v \pi \left(\frac{d}{2}\right)^2 \end{cases} \quad (1)$$

Where ρ is the density of pipeline fluids (unit: Kg/m^3), v is the velocity of pipeline fluids (unit: m/s), d is the pipe diameter (unit: m), Q is the pipeline flow rate (unit: m^3/h) and η is the kinetic viscosity of liquids (unit: $\text{Pa}\cdot\text{s}$). The experiment was performed in the condition of the indoor temperature of $20^\circ\text{C}\sim 25^\circ\text{C}$. The kinetic viscosity of pure water medium is $1.005\times 10^{-3}\text{Pa}\cdot\text{s}$. Besides, the kinetic viscosity of carbonate pipeline fluids is $1.6\times 10^{-3}\text{Pa}\cdot\text{s}$ thanks to consider of minerals in the pipeline liquids.

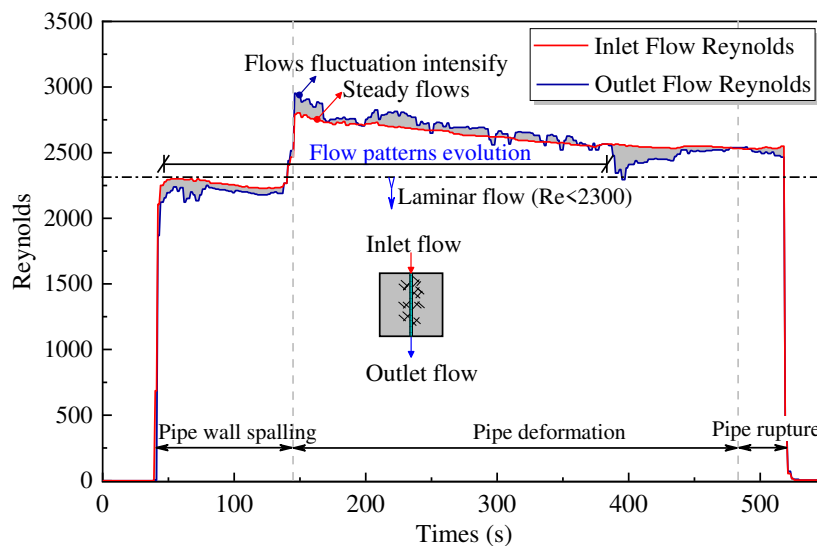


Figure 8 Evolution of the flow regime of the pipe fluid during the rupture of the karst rock specimen

It is well known that the pipe flow regime can gradually transform into another state with the carbonate rock failures. The pipe-wall will be spalling with the fluids flow in carbonate rocks. The experiment data prove that the pipe flow regime is dominated by the laminar flow that the Reynolds number of pipeline fluids is less than 2300 at the cracks initiation. Then, the flow rate of pipeline fluids gradually changes to the transitional regime that the Reynolds number ranges from 2300 to 4000, and even beyond of 4000 that to be the turbulent flow, due to the intensified fracture and the damaged pipe. With respect to the failure pattern, the failure type of carbonate rocks in the conditions of the hydro-conductivity of pipeline show the brittle behaviour. In order to further quantify the non-linear evolutions of PF-FF, the X-ray image obtaining from the experiment is post-processed by the LOG algorithm. Features of liquids in fractures extracted from the LOG images and its fractal dimension are calculated using boxing counting method. The fractal dimension (D_f) of liquids in fractures changes with the transition from pipe flow to fissure flow during carbonate rock failures, which is shown in Figure 9.

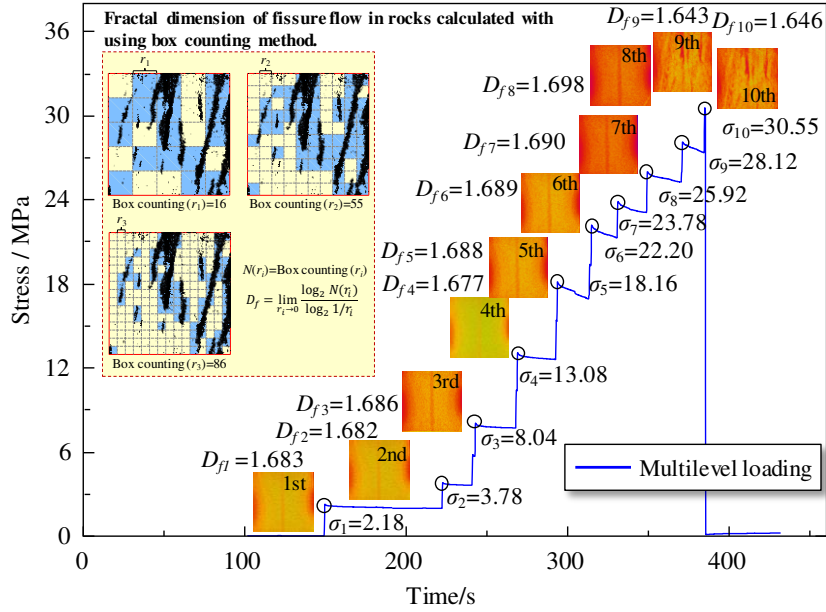


Figure 9 The fractal dimension of liquids in fractures changes with the multi-level loadings

It can be learned from the Figure 9 that fractal dimensions of PF to FF with the multi-level loading has a tendency to decrease abruptly, which indicates that the evolution process experiences from the laminar flow to the transitional flow. Therefore, the flow regime of pipelines will be changed with the rock failures before landslides. In fact, the flow rate of upstream and downstream can be traced for making decision on the pre-warning of landslide disaster.

3.2 Hydro-damage properties of RBM failures induced by hydrodynamics

Some disasters are always frequent to happen in the red bed mudstone (RBM) region. This is due to the RBM containing abundance of clay minerals such as kaolinite and montmorillonite, which will aggravate the softening and disintegration when coupled with the water (Wu et al. 2018). In the engineering, slopes of highway are eroded by the heavy rainfall and easily form water-conducting trenches. Meanwhile, the formed hydrodynamics conditions will result in the slopes instability in the RBM regions. Therefore, some engineering problems threats to the safety operation of highways such as the destroyed anchor frame beam, the bolt reinforcement failures and so on. In order to accurately evaluate the slopes stability of the RBM regions, the damage testing of mudstone rock materials under hydrodynamics is carried out. These results can provide some theoretical guidance for the pre-warning of geo-disasters in the RBM regions.

The damaged properties of RBM will be aggravated under hydrodynamics, which is the essential cause of slope instability. The classical damage mechanics present that the damage coefficient of brittle materials can be defined with using elastic strain methods and the formula is as follows:

$$D = 1 - \frac{E'}{E_0} \quad (2)$$

Where E_0 is the initial elastic modulus of material (unit: MPa), E' is the elastic modulus of damaged material. On the basis of this definition, this paper presents the elastic modulus of hydro-damage materials as E'_s . Hence, the damage coefficient of RBM rock materials expressed as below.

$$D = 1 - \frac{E'_s}{E_0} \quad (3)$$

Where E'_s/E_0 is the ratio of the elastic modulus of hydro-damaged rocks and undamaged rocks. The tests in

this paper can obtain X-ray images of hydro-damaged RBM rocks. The different components of liquids and rock matrix are to the certain X-ray absorption attenuation what the different tissues and organs are to different X-ray absorption doses. Thus, X-ray absorption thresholds are used to extract image features of the different components of RBM materials. The pixel window with a fixed size of 824×1087 is set for analyzing X-ray images. Recording the accumulated values of X-ray absorptions with respect to the n^{th} load, I_c represent the X-ray absorption values of crack in rocks and I_m represent the X-ray absorption values of rock matrixes.

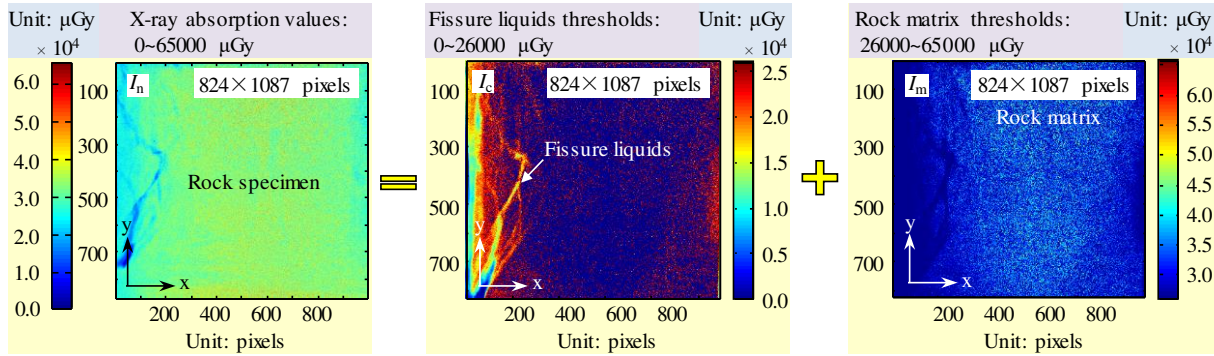


Figure 10 Image features quantified with the different components of RBM using X-ray absorption thresholds

Some published literatures have proved that the X-ray absorption values of I_n is related to integrity and strength of rocks, i.e. parameters of E_s , E'_s separately has the functional relationship with I_n , where $I_n = I_c + I_m$, the data examine that I_m is far more than I_c . Therefore, Equation 4 can be inferred as below.

$$D = 1 - \frac{I_m}{I_0} \quad (4)$$

Where I_m represents the total X-ray absorption values of the unsaturated rocks (unit: μGy), I_0 represents the total X-ray absorption values of the initial rocks (unit: μGy) and D is the hydro-damage coefficient of rocks. Also, I_c is the total X-ray absorption values of crack and fracture in rocks. According to different compositions of rocks in the X-ray images, I_c thresholds of RBM-01 specimen sets to be less than $26000 \mu\text{Gy}$, of RBM-02 and RBM-03 are set to be less than $19000 \mu\text{Gy}$. I_c and I_m analyzed of RBM specimens statistically using MATLAB as shown in Figure 11. Finally, the hydro-damage coefficient D could be calculated by the analyzed image data.

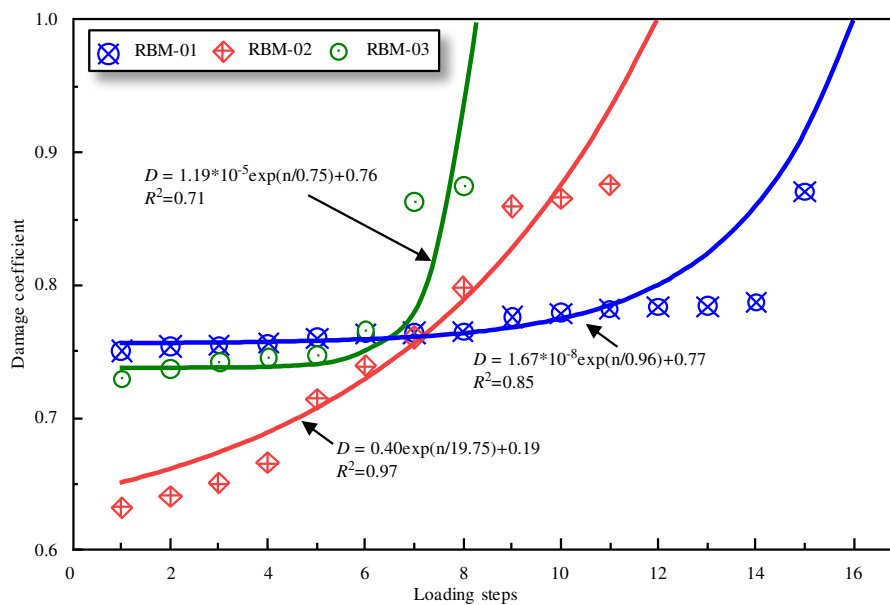


Fig. 11 The hydro-damage coefficient variations with rock failures of RBM under hydrodynamics

It can be observed from the Figure 11 that hydro-damage coefficients show an exponential increasing with the multilevel stress loadings. This indicates that the coupled stress and hydrodynamics aggravate the damaged rate of RBM. To be specific, the external stress causes fractures expansion in rocks, then the water filling fractures will be driven by hydrodynamics pressure, this means fluids pressure of pores and fractures will be increasing sharply. Therefore, the damage degree of RBM will be intensified together with the crack propagation and fractures flow, showing dual behavior of nonlinear seepage and anomalous diffusion effects. Therefore, this study defines the coefficient of seepage and diffusion (C_d) to quantitatively describe the dual mechanical properties of seepage and diffusion in rocks, and the pixels number is counted for different feature areas in X-ray images. Equation 5 is proposed to calculate the C_d values as below.

$$C_d = \frac{S_{total}}{N_{pixels}} \cdot \frac{N_c}{t} \quad (5)$$

Where C_d is the coefficient of seepage and diffusion (unit: mm^2/s), this means the areas of water seepage and diffusion with water filling fractures in rocks at square millimeter per seconds. S_{total} is the total calculated features segmentation areas in the X-ray image (unit: mm^2), N_{pixels} is the pixels number of the certain feature area in the X-ray image of rocks, N_c is the pixels number of damaged area of rocks, and t is the time of RBM specimens under hydro conductivity duration (unit: s).

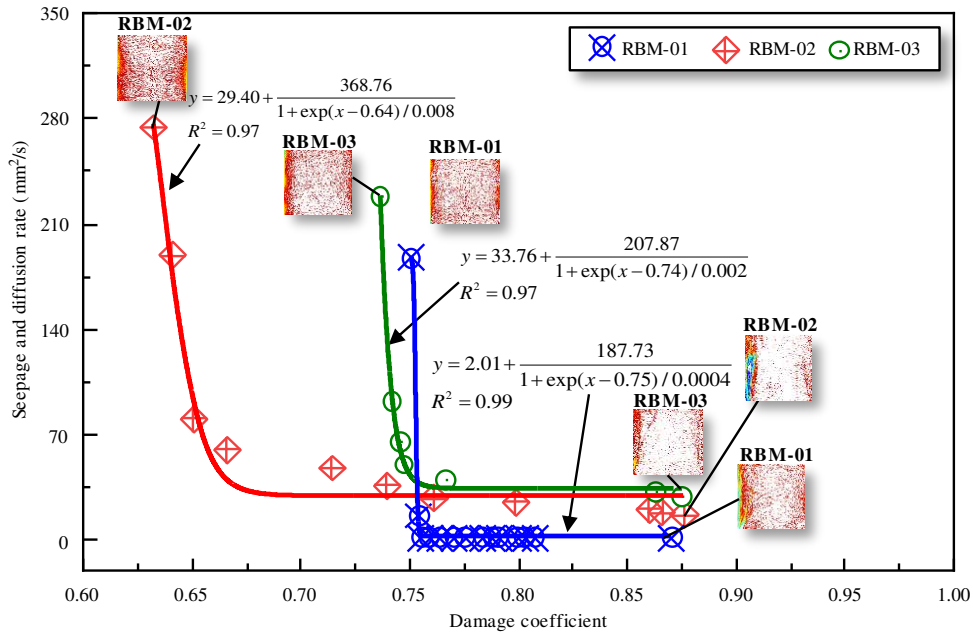


Figure 12 Hydro-damage coefficient evolutions of RBM specimens under hydrodynamics and multilevel stress loadings

Figure 12 is given by the Boltzmann function of mathematical fitting relations of the hydro-damage (D) and seepage diffusion coefficient (C_d), this indicates that C_d tends to be non-linearly decreasing as the intensified damage of rocks. Initially, the intact RBM has a high permeability and larger diffusion coefficient. Therefore, the initial hydro-properties of RBM rocks should be enhanced for resisting catastrophe induced by rain falling, which is the key point for ensuring slope stability and bolting support in the engineering.

3.3 Bursting disaster induced by fissure water in the goaf of coal mine

The fractures enrich in the overlying stratum and further develop with coal seams mining (Sun et al. 2020a). Broken coals and rocks of enrich fractures store easily a large of groundwater in the goaf, which involves the

essential scientific issues of nonlinear flow and diffusion effects. Therefore, some physical equations are proposed necessarily for describing the catastrophe process of groundwater bursting, which is of great significance for proposing the hydro-geo-dynamics theory and hazards prevention.

From 1879 to 1955, Albert Einstein published a series of papers involving modern physics, in which described microscopic particle motion, immersed in liquid and derived the diffusion equation. These results prove that the particle waves are related to the Gaussian distribution, the mean square displacement (MSD) has the functions of particle diffusion motion with the time as below.

$$\text{MSD} = \langle (r - \langle r \rangle)^2 \rangle \propto t \quad (6)$$

Where r is the relative displacement of particle diffusion, and $\langle r \rangle^2$ represents the average of mean square displacement of particles (unit: s).

In fact, the fluids in fractures and its distribution are always in a dynamic system. The micro-dynamic theory mainly defines the motion model of molecules or atoms in liquids on the basis of relationship between the MSD and time. Therefore, we believe that the motion model of water molecules in solid rocks can be described by the mean square value. For considering the valid flow rate, this study proposes the mean square flow (MSF) to quantify the increased flow in fractures with time. In other words, MSF should be determined with the magnitude stress or the time. For this purpose, the experiment on flow visualization during coal and rock failures has been carried out. The analyzed results focus on X-ray image data of fluids in rock fractures and acoustic emission (AE), of the stress loading related to time directly. Also, the pixels number N_n of feature areas of fissure water in the X-ray image is account using thresholds segmentation. The more pixels number corresponds to the bigger areas of fissure water, i.e. $Q_n \propto N_n$. Finally, the flow and diffusion of fissure water in rocks can be described as the MSF with the function of the time, as shown in Equation 7.

$$\text{MSF} = \frac{1}{N} \sum_{n=1}^N (Q_{n+1} - Q_n)^2 \quad (7)$$

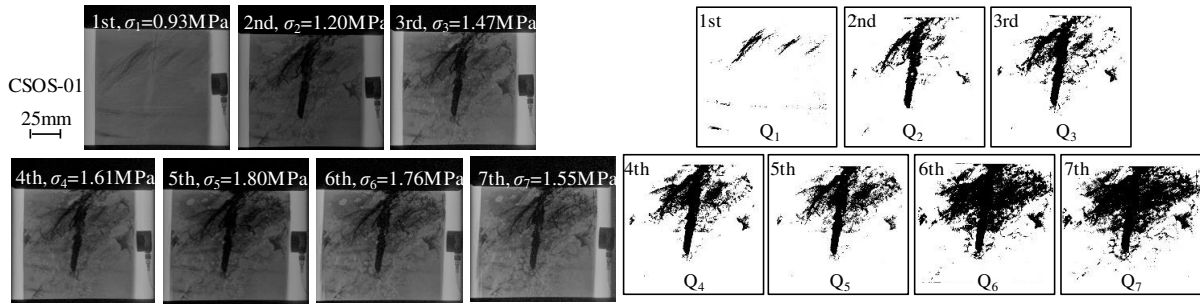
Where Q_n is the flow rate of fissure fluids of rocks under the n^{th} loading (unit: mL). It can be calculated by the flow visualization experiment of fissure water in rocks of X-ray images. The total number of pixels is defined as N_1, N_2, \dots, N_n .

Felicity effect defines the fracture degree of rock specimens during the test using AE ([Zhang et al. 2017](#)). That means the AE signal is no longer intensifies when loading stress of material exceeds the previous maximum value. Felicity effect is defined as the ratio between the AE onset stress and maximum of the previous stress as shown in Equation 8.

$$FR_{(\sigma)} = \frac{\sigma_{\text{AE}}}{\sigma_{\text{max}}} \quad (8)$$

Where σ_{AE} and σ_{max} are, respectively, the AE onset stress and the maximum of the previous stress, and $FR(\sigma)$ is the felicity ratio calculated by the multilevel stress loading.

The experiment can obtain the X-ray image of fissure water in coals and rocks as shown in Figure 13a, and the features of fissure water flow extracted from the X-ray image use thresholds segmentation method as shown in Figure 13b. Finally, the fractional exponent relationship between MSF and failure degree is given as the double logarithmic curves, which is shown in Figure 14.



(a) X-ray images of fissure water (b) Features of fissure water flow and diffusion

Figure 13 Features extraction of flow and diffusion of fissure water using thresholds segmentation

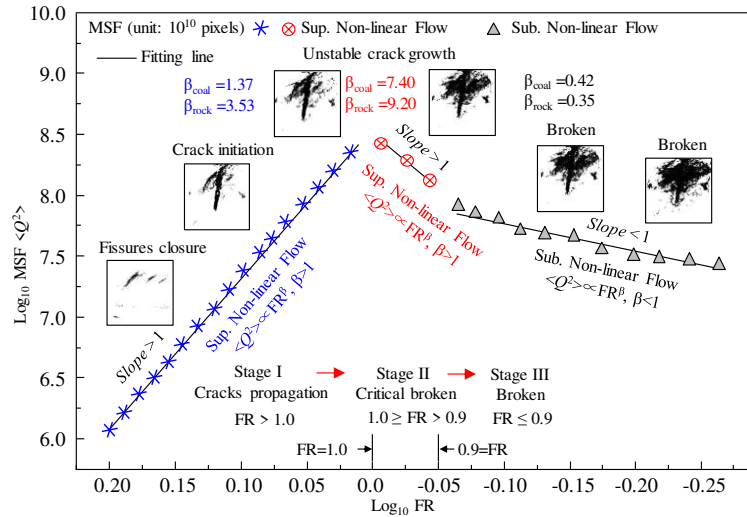


Figure 14 Logarithmic relations between MSF and AE Felicity ratio during rock failures

It can be observed from Figure 14 that the fractional exponent relations of MSF and FR. If β is more than 1, the flow rate of fissure water shows the super flow and diffusion regime. In contrast, if β is less than 1, the flow and diffusion in coals and rocks are super regime. When β is equal to 1, the flow rate of fissure water shows the linear flow and diffusion phenomenon. To be more specific, the fractional index (β) of MSF and FR is 1.37 at the initial stage. As the development of coal failures, the fractional index (β) of MSF and FR reaches at 7.40. Finally, the fractional index (β) of MSF and FR is falling down to 0.42. For mudstone rocks, the fractional index (β) of MSF and FR are 3.53, 9.20 and 0.35, respectively. Therefore, the fractional index of β can be used to quantify flow regime of fissure water that induced disaster relating to coal and rock failure degree in the goaf.

4. Discussion

This study proposes a new method for observing fluid in rock fractures using the enhanced X-ray image of digital radiography on the basis of block material scale. Three types of rock prepared for the experiment, aiming at exploring the multi-behaviors of seepage, damage and diffusion in rocks. On the basis of obtaining multi-source data of rock failures, this study places a strong connection between the nonlinear flow of fissure water and the rock strength. These results provide some theoretical guidance for geo-disasters induced by the interactions of water and rock in the engineering.

As well as known, any experiment methods all have limitations for exploring essential problems of rocks. This proposed method is only suitable for water-rock interaction based on the material scale. After this experiment, we find that three aspects of following need to be improved.

(1) The X-ray scanning system platform should be upgraded for further to obtain the more resolution images. The experiment in this study is carried out with the flat panel type of X-ray DR platform. Industrial CT (μ -CT) or medical CT (m-CT) scanning could be used for obtaining volume data.

(2) The pressure cell of rocks should be designed of approving rigidity and radiolucent requirements. In this experiment, the specimen is wrapped in plastic films. Once the specimen is broken, which is also results in the film leakage. These mistakes in the experiment will affect the collection of test data. Therefore, the pressure cell of rocks should be given as the satisfied designs for sealed, rigid and radiolucent materials.

(3) The high-performance loading device should be developed for the static and dynamics. In this experiment, we use the hydraulic jack to realize the path of multilevel stress loading on rocks. The stress path of experiment is matched with the blasting load, disturbance load of excavation and so on.

5. Conclusion

The new proposed method in this paper have been applied for researching on three aspects of hydro-dynamics theory, mainly involving the fundamental theory of large-scale landslides in karst mountains of southwestern China, slope instability induced by rainfall in RBM regions and hydro disasters of groundwater bursting in the goaf of coal mine. Some significant conclusions are as below.

(1) The precursory behaviors of landslides in karst region are pipe rupture due to the alternated flow. Flow regime of karst pipe can be used for determining large-scale collapse of mountain. The flow regime of karst pipe changes from the laminar flow to the transitional flow or turbulent flow. Thus, in regard to practical methods for predicting karst geological disasters, the Q values for the upstream and downstream of karst pipes and flow-regime can be determined to the pre-warnings of karst landslides.

(2) The slope instability of red-bed mudstone (RBM) is due to the damaged rock mass under hydrodynamics relating to the seepage and diffusion effects. In this study, the proposed experimental method can evaluate the damage properties of RBM on the basis of X-ray images using thresholds segmentation. The results show that the seepage diffusion coefficient (C_d) tends to be non-linearly decreasing as the intensified damage of RBM rocks. Therefore, the initial hydro-properties of RBM rocks should be enhanced for resisting catastrophe induced by rain falling, which is the key point for ensuring slope stability and bolting support in the engineering.

(3) Groundwater bursting from the goaf induced by fissure water flow changing with coal seams mining involves nonlinear flow and diffusion effects. The experiment proves that the mean square flow of fissure water has the fractional functions with the failure degree of coals and rocks. Therefore, the fractional index of β can be used to quantify flow regime of fissure water that induces disaster relating to coal and rock failure degree in the goaf.

Acknowledgments

This study was supported by the National Key Research and Development Program (Approval No. 2018YFC1504801 and 2018YFC1504902), the Open Research Fund Program of State Key Laboratory of Hydroscience and Engineering (Approval No. sklhse-2021-C-02), the Scientific Research Foundation of Hainan University (Approval No. KYQD (ZR)-20104), and the General Program of China Postdoctoral Science Foundation (Approval No. 2018M 641370).

Compliance with Ethical Standards

Conflict of interest The authors declare that they have no conflicts of interest in this study. The authors certify that

they have no commercial or associative interest that represents a conflict of interest in connection with the paper submitted.

Reference

- Adji, T.N. & Bahtiar, I.Y. (2016) Rainfall-discharge relationship and karst flow components analysis for karst aquifer characterization in Petoyan Spring, Java, Indonesia. *Environmental Earth Sciences* **75**: <https://doi.org/10.1007/s12665-016-5553-1>
- Barton, N., Bandis, S. & Bakhtar, K.: Strength, deformation and conductivity coupling of rock joints. *Journal* **22**, 121-140 (1985). [https://doi-org.s12040.top/10.1016/0148-9062\(85\)93227-9](https://doi-org.s12040.top/10.1016/0148-9062(85)93227-9)
- Chechkin, A.V., Gorenflo, R. & Sokolov, I.M. (2005) Fractional diffusion in inhomogeneous media. *Journal of Physics A: Mathematical and General* **38**: L679. <https://doi.org/10.1088/0305-4470/38/42/L03>
- Chen, Y., Hu, S., Wei, K., et al. (2014) Experimental characterization and micromechanical modeling of damage-induced permeability variation in Beishan granite. *International Journal of Rock Mechanics and Mining Sciences* **71**: 64-76. <https://doi.org/10.1016/j.ijrmms.2014.07.002>
- Gao, Y., Li, B., Gao, H.Y., et al. (2020) Dynamic characteristics of high-elevation and long-runout landslides in the Emeishan basalt area: a case study of the Shuicheng "7.23" landslide in Guizhou, China. *Landslides* **17**: 1663-1677. <https://doi.org/10.1007/s10346-020-01377-8>
- Ghosh, A. & Daemen, J.J.K. (1993) Fractal characteristics of rock discontinuities. *Engineering Geology* **34**: 1-9. [https://doi.org/10.1016/0013-7952\(93\)90039-f](https://doi.org/10.1016/0013-7952(93)90039-f)
- Hirono, T., Takahashi, M. & Nakashima, S. (2003) In situ visualization of fluid flow image within deformed rock by X-ray CT. *Engineering Geology* **70**: 37-46. [https://doi.org/10.1016/s0013-7952\(03\)00074-7](https://doi.org/10.1016/s0013-7952(03)00074-7)
- Ju, Y., Liu, P., Ren, Z., et al. (2021) Characterization of stress field evolution during 3D internal fracture propagation using additively printed models and frozen stress techniques. *Theoretical and Applied Fracture Mechanics* **111**: <https://doi.org/10.1016/j.tafmec.2020.102870>
- Ju, Y., Zhang, Q., Yang, Y., et al. (2013) An experimental investigation on the mechanism of fluid flow through single rough fracture of rock. *Science China Technological Sciences* **56**: 2070-2080. <https://doi-org.s12040.top/10.1007/s11431-013-5274-6>
- Lavrov, A. (2014) Radial flow of non-newtonian power-law fluid in a rough-walled fracture: effect of fluid rheology. *Transport in Porous Media* **105**: 559-570. <https://doi.org/10.1007/s11242-014-0384-6>
- Liu, R., Huang, N., Jiang, Y., et al. (2020) A numerical study of shear-induced evolutions of geometric and hydraulic properties of self-affine rough-walled rock fractures. *International Journal of Rock Mechanics and Mining Sciences* **127**: 104211. <https://doi.org/10.1016/j.ijrmms.2020.104211>
- Liu, R.C., Jing, H.W., He, L.X., et al. (2017) An experimental study of the effect of fillings on hydraulic properties of single fractures. *Environmental Earth Sciences* **76**: <https://doi.org/10.1007/s12665-017-7024-8>
- Liu, X., Wang, E., Wang, S., et al. (2008) Representation method of fractured rock mass and its hydraulic properties study. *Chinese Journal of Rock Mechanics and Engineering* **27**: 1814-1821. <https://kns.cnki.net/kcms/detail/detail.aspx?FileName=YSLX200809010&DbName=CJFQ2008>
- Raghavan, R. (2011) Fractional derivatives: Application to transient flow. *Journal of Petroleum Science and Engineering* **80**: 7-13. <https://doi.org/10.1016/j.petrol.2011.10.003>
- Rong, G., Hou, D., Yang, J., et al. (2017) Experimental study of flow characteristics in non-mated rock fractures considering 3D definition of fracture surfaces. *Engineering Geology* **220**: 152-163. <https://doi.org/10.1016/j.enggeo.2017.02.005>
- Rong, G., Yang, J., Cheng, L., et al. (2018) A Forchheimer equation-based flow model for fluid flow through rock fracture during shear. *Rock Mechanics and Rock Engineering* **51**: 2777-2790. <https://doi.org/10.1007/s00603-018-1497-y>

- Shahbazi, A., Saeidi, A. & Chesnaux, R. (2020) A review of existing methods used to evaluate the hydraulic conductivity of a fractured rock mass. *Engineering Geology* **265**: <https://doi.org/10.1016/j.enggeo.2019.105438>
- Sun, H., Liu, X., Ye, Z., et al. (2021) Experimental investigation of the nonlinear evolution from pipe flow to fissure flow during carbonate rock failures. *Bulletin of Engineering Geology and the Environment* **1-12**.
<https://doi.org/10.1007/s10064-021-02210-9>
- Sun, H., Liu, X., Zhang, S., et al. (2020a) Experimental investigation of acoustic emission and infrared radiation thermography of dynamic fracturing process of hard-rock pillar in extremely steep and thick coal seams. *Engineering Fracture Mechanics* **226**: 106845. <https://doi.org/10.1016/j.engfracmech.2019.106845>
- Sun, H., Liu, X. & Zhu, J. (2019) Correlational fractal characterisation of stress and acoustic emission during coal and rock failure under multilevel dynamic loading. *International Journal of Rock Mechanics and Mining Sciences* **117**: 1-10. <https://doi.org/10.1016/j.ijrmms.2019.03.002>
- Sun, Z.H., Wang, L.Q., Zhou, J.Q., et al. (2020b) A new method for determining the hydraulic aperture of rough rock fractures using the support vector regression. *Engineering Geology* **271**:
<https://doi.org/10.1016/j.enggeo.2020.105618>
- Wang, L., Liu, J.F., Pei, J.L., et al. (2015) Mechanical and permeability characteristics of rock under hydro-mechanical coupling conditions. *Environmental Earth Sciences* **73**: 5987-5996. <https://doi.org/10.1007/s12665-015-4190-4>
- Wang, Y., Li, X., Zheng, B., et al. (2016) Experimental study on the non-Darcy flow characteristics of soil-rock mixture. *Environmental Earth Sciences* **75**: <https://doi.org/10.1007/s12665-015-5218-5>
- Wang, Z.H., Xu, C.S. & Dowd, P. (2018) A Modified Cubic Law for single-phase saturated laminar flow in rough rock fractures. *International Journal of Rock Mechanics and Mining Sciences* **103**: 107-115.
<https://doi.org/10.1016/j.ijrmms.2017.12.002>
- Wang, Z.H., Xu, C.S. & Dowd, P. (2019) Perturbation Solutions for Flow in a Slowly Varying Fracture and the Estimation of Its Transmissivity. *Transport in Porous Media* **128**: 97-121.
<https://doi.org/10.1007/s11242-019-01237-7>
- Watson, F., Maes, J., Geiger, S., et al. (2019) Comparison of Flow and Transport Experiments on 3D Printed Micromodels with Direct Numerical Simulations. *Transport in Porous Media* **129**: 449-466.
<https://doi.org/10.1007/s11242-018-1136-9>
- Wu, L.Z., Zhang, L.M., Zhou, Y., et al. (2018) Theoretical analysis and model test for rainfall-induced shallow landslides in the red-bed area of Sichuan. *Bulletin of Engineering Geology and the Environment* **77**: 1343-1353.
<https://doi.org/10.1007/s10064-017-1126-0>
- Wu, Q., Wang, M. & Wu, X. (2004) Investigations of groundwater bursting into coal mine seam floors from fault zones. *International Journal of Rock Mechanics and Mining Sciences* **41**: 557-571.
<https://doi.org/10.1016/j.ijrmms.2003.01.004>
- Xie, L.Z., Gao, C., Ren, L., et al. (2015) Numerical investigation of geometrical and hydraulic properties in a single rock fracture during shear displacement with the Navier-Stokes equations. *Environmental Earth Sciences* **73**: 7061-7074. <https://doi.org/10.1007/s12665-015-4256-3>
- Xiong, F., Jiang, Q., Xu, C., et al. (2019) Influences of connectivity and conductivity on nonlinear flow behaviours through three-dimension discrete fracture networks. *Computers and Geotechnics* **107**: 128-141.
<https://doi.org/10.1016/j.compgeo.2018.11.014>
- Xiong, F., Wei, W., Xu, C., et al. (2020) Experimental and numerical investigation on nonlinear flow behaviour through three dimensional fracture intersections and fracture networks. *Computers and Geotechnics* **121**: 103446.
<https://doi.org/10.1016/j.compgeo.2020.103446>
- Yao, M., Liu, P.G., Shang, M.T., et al. (2016) Determining sources of mine water based on hydraulic characteristics analysis of a fault system. *Environmental Earth Sciences* **75**: <https://doi.org/10.1007/s12665-016-5660-z>

- Zhang, M., Yin, Y. & Huang, B. (2015) Mechanisms of rainfall-induced landslides in gently inclined red beds in the eastern Sichuan Basin, SW China. *Landslides* **12**: 973-983. <https://doi.org/10.1007/s10346-015-0611-4>
- Zhang, Y., Chen, Y., Yu, R., et al. (2017) Effect of loading rate on the felicity effect of three rock types. *Rock Mechanics and Rock Engineering* **50**: 1673-1681. <https://doi.org/10.1007/s00603-017-1178-2>
- Zhao, W.S., Picard, G., Leu, G., et al. (2010) Characterization of single-phase flow through carbonate rocks: Quantitative comparison of NMR flow propagator measurements with a realistic pore network model. *Transport in Porous Media* **81**: 305-315. <https://doi.org/10.1007/s11242-009-9402-5>
- Zhou, X.-P. & Xiao, N. (2018) A hierarchical-fractal approach for the rock reconstruction and numerical analysis. *International Journal of Rock Mechanics and Mining Sciences* **109**: 68-83. <https://doi.org/10.1016/j.ijrmms.2018.06.016>
- Zhou, X.-P. & Xiao, N. (2019) Analysis of fracture properties of three-dimensional reconstructed rock model using hierarchical-fractal annealing algorithm. *Engineering Geology* **256**: 39-56. <https://doi.org/10.1016/j.enggeo.2019.04.017>
- Zhu, J.B., Zhou, T., Liao, Z.Y., et al. (2018) Replication of internal defects and investigation of mechanical and fracture behaviour of rock using 3D printing and 3D numerical methods in combination with X-ray computerized tomography. *International Journal of Rock Mechanics and Mining Sciences* **106**: 198-212. <https://doi.org/10.1016/j.ijrmms.2018.04.022>
- Zimmerman, R.W. & Bodvarsson, G.S. (1996) Hydraulic conductivity of rock fractures. *Transport in Porous Media* **23**: 1-30. <https://doi-org.s12040.top/10.1007/BF00145263>

Figures

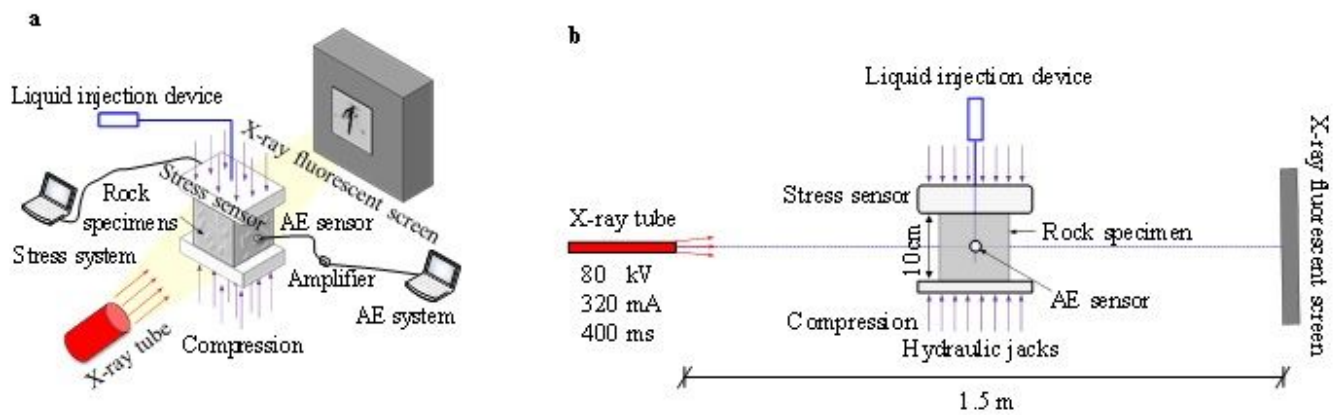


Figure 1

(a) Three-dimensional schematic of the design principle (b) Principle of observing fluid in rock fractures using EXIDR

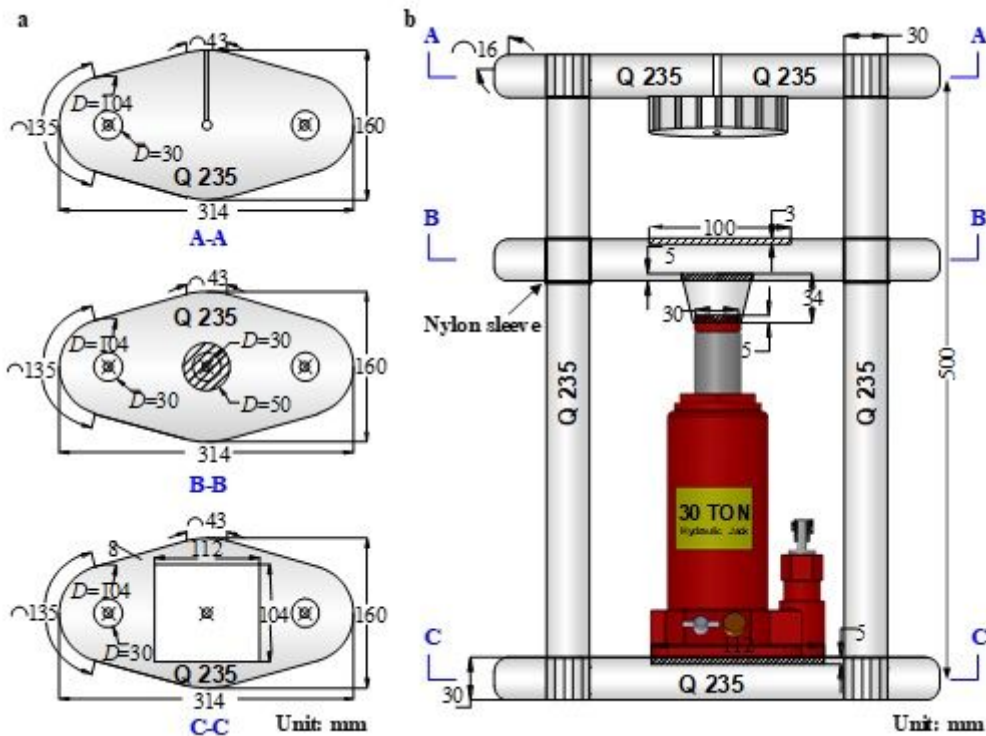


Figure 2

Design of multi-level loading device matching with X-ray DR or CT system



Figure 3

Monitoring components for the testing platform system (a) Self-priming pump of LS-0412 (b) Stress sensor (c) Flow sensor of DN4

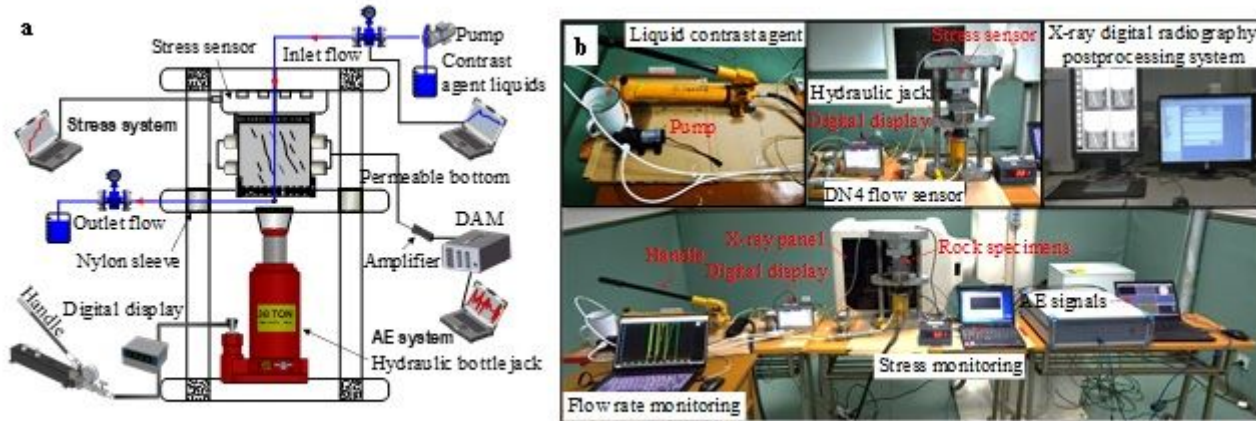


Figure 4

Physical platform and testing system of observing fluid in rock fractures using EXIDR (a) Test system design (b) Physical platform



Figure 5

Standard preparations of rock specimens of different lithology. (a) Karst rock specimen (b) red bed mudstone specimen (c) Coal rock specimen

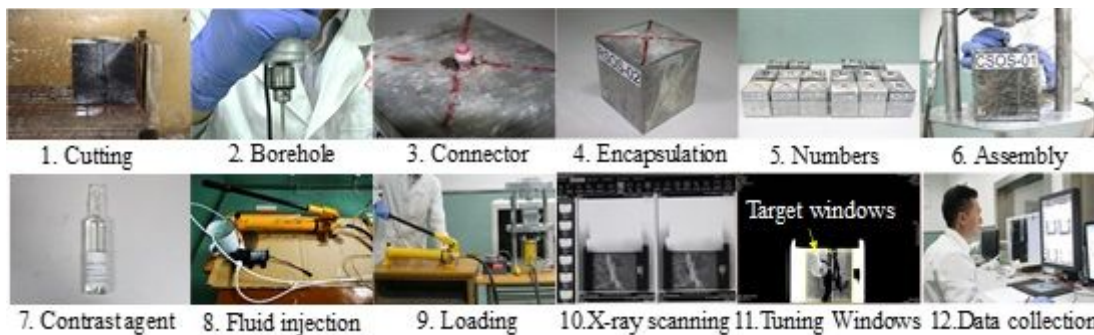


Figure 6

Experiment steps of visualization fluid in fractures during rock failures using X-ray digital radiography.

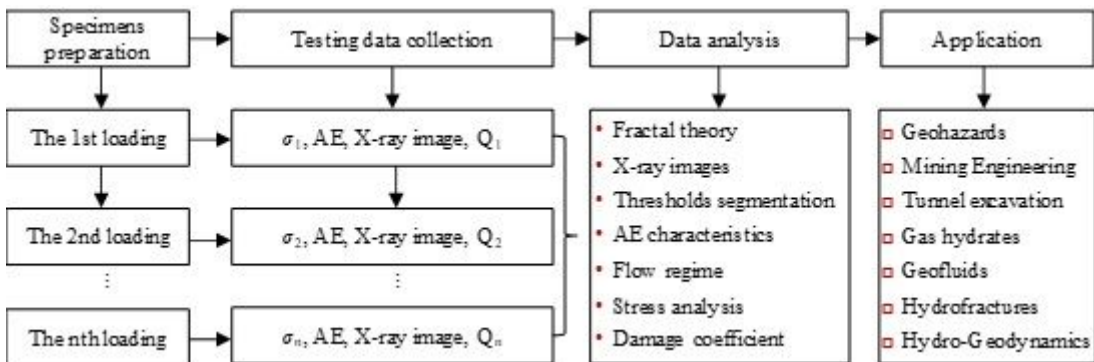


Figure 7

Fracture fluid evolution analysis method and application field during rock fracture

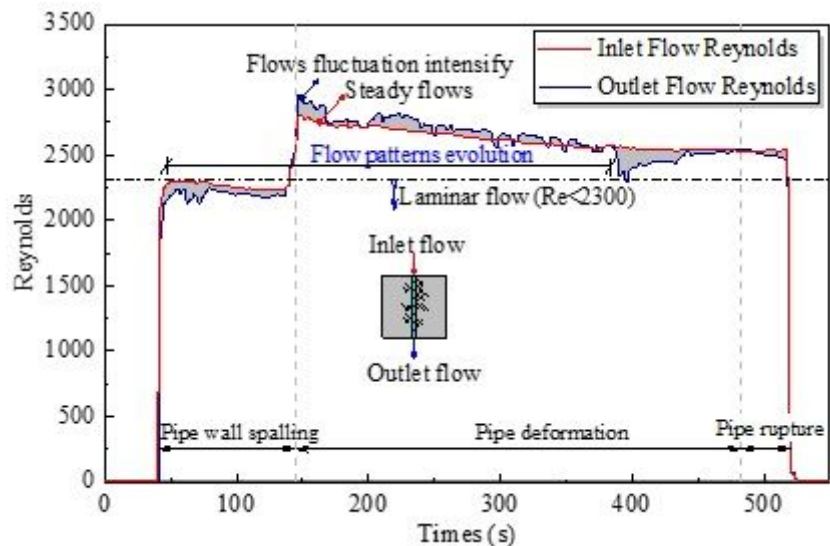


Figure 8

Evolution of the flow regime of the pipe fluid during the rupture of the karst rock specimen

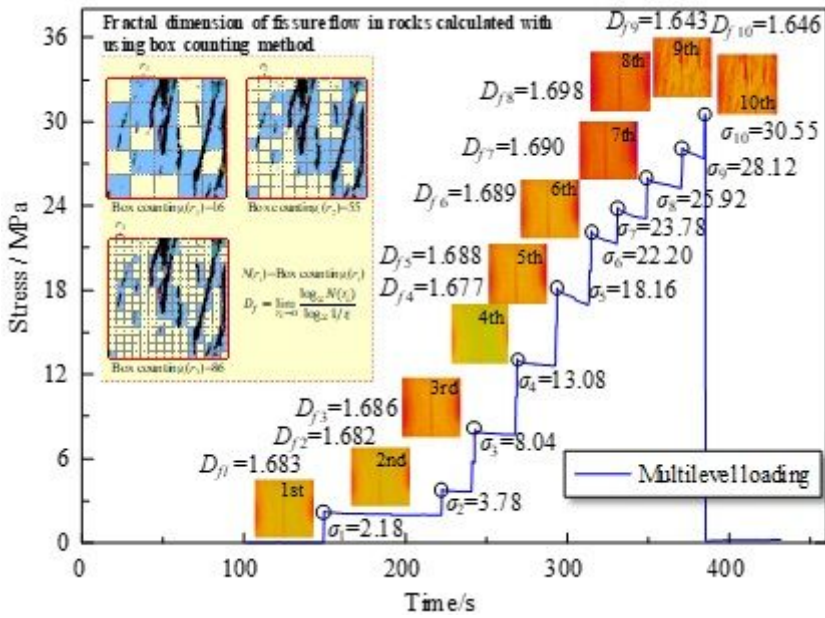


Figure 9

The fractal dimension of liquids in fractures changes with the multi-level loadings

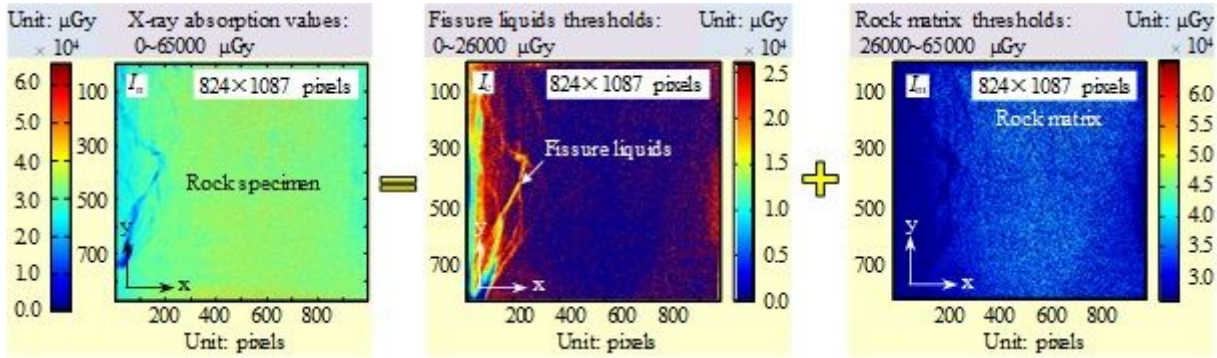


Figure 10

Image features quantified with the different components of RBM using X-ray absorption thresholds

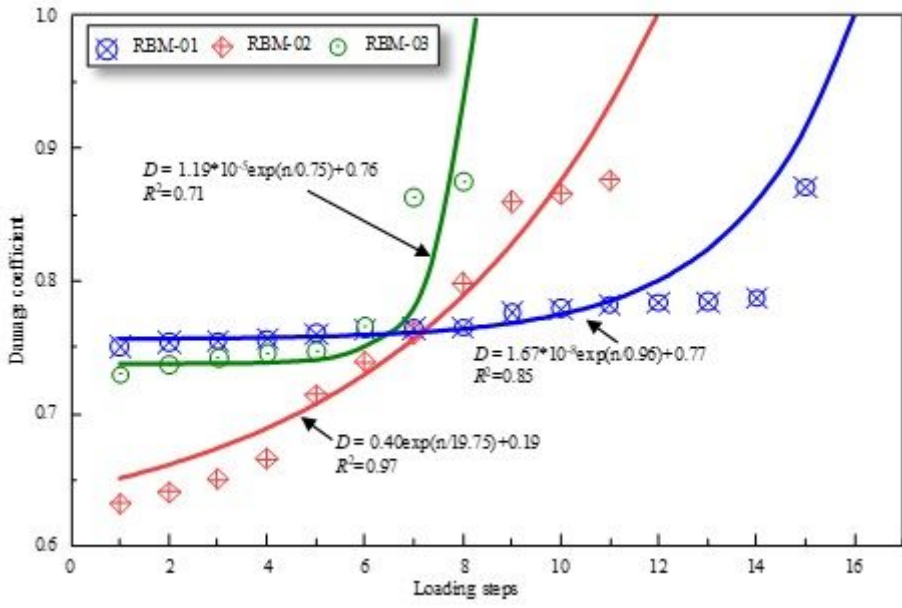


Figure 11

The hydro-damage coefficient variations with rock failures of RBM under hydrodynamics

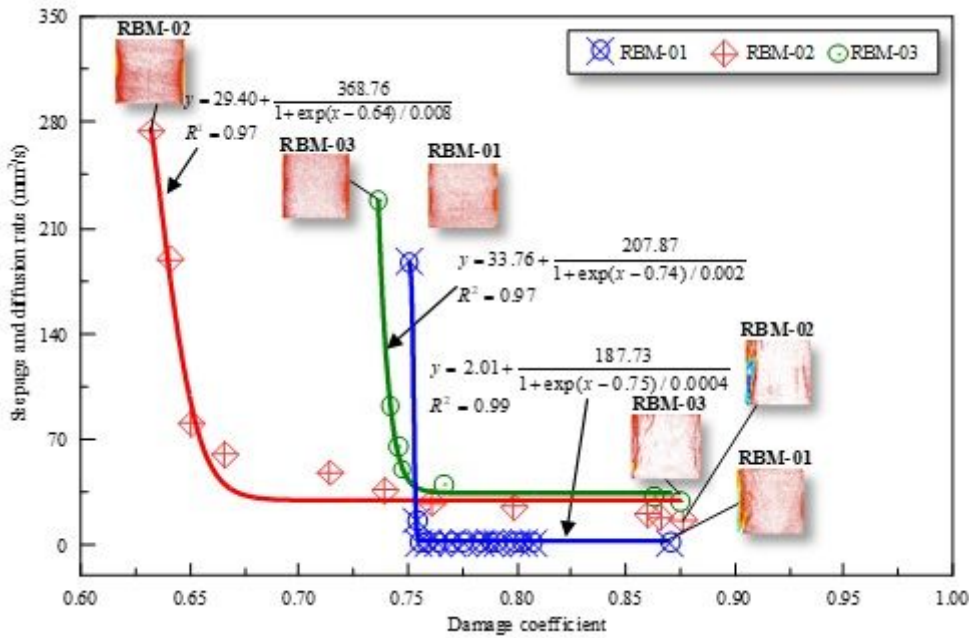


Figure 12

Hydro-damage coefficient evolutions of RBM specimens under hydrodynamics and multilevel stress loadings

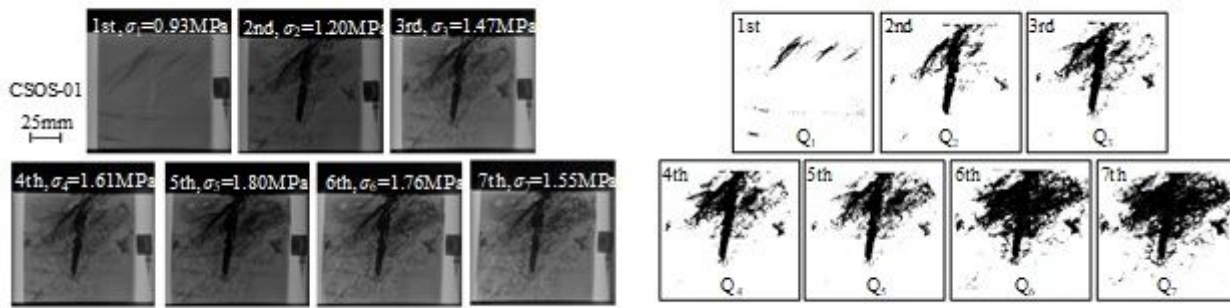


Figure 13

Features extraction of flow and diffusion of fissure water using thresholds segmentation. (a) X-ray images of fissure water (b) Features of fissure water flow and diffusion

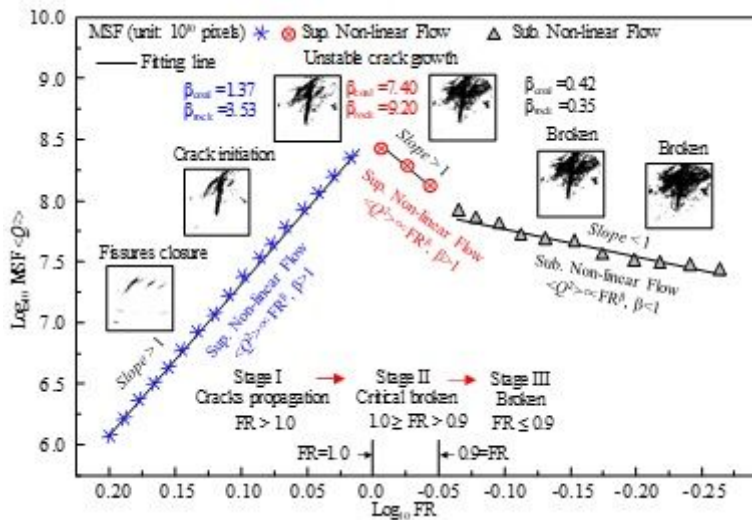


Figure 14

Logarithmic relations between MSF and AE Felicity ratio during rock failures